International Journal on Recent and Innovation Trends in Computing and Communication
ISSN: 2321-8169 Volume: 11 Issue: 11
Article Received: *10 September 2023* ***Revised:*** *20 October 2023* ***Accepted:*** *30 October 2023*

Parallel Complementary Virtual Arrays Algorithm for Direction of Arrival (DOA) Estimation

Sanjeev Kumar Machkuri, Y Ravi Kumar

Dept. of ECE, Mahatma Gandhi Institute of Technology, Hyderabad, Telangana, India

Scientist-G(Retd), DLRL DRDO, Hyderabad, Telangana, India

E-mail; msanjeevkumar_ece@mgit.ac.in, dr.ravikumaryeda@gmail.com

Abstract

This Paper discusses the challenges faced by previous method 2D Direction of Arrival (DOA) systems, such as low degrees of freedom, poor resolution, and significant estimation errors in scenarios with small snapshots. In response to these issues, the present method proposes a low-complexity 2D Direction of Arrival (DOA) estimation algorithm based on a parallel complementary virtual array.

The algorithm utilizes two mutually parallel complementary linear arrays to generate a virtual array, addressing the limitations of traditional parallel arrays. It constructs an extended matrix with enhanced 2D angular degrees of freedom using covariance and cross-covariance matrices. The final step involves obtaining automatic matching 2D angle estimates through Singular Value Decomposition (SVD) and Estimation of Signal Parameters via Rotational Invariance Techniques (ESPRIT).

In comparison to traditional 2D DOA estimation methods, the proposed algorithm better exploits the information from the array's received data. It can identify more incoming signals, offering high resolution without the need for 2D linear search or angle parameter matching. Importantly, it demonstrates effective estimation even in scenarios with low Signal-to-Noise Ratio (SNR) and small snapshots. Experimental simulation results validate the effectiveness and reliability of the proposed algorithm.

1.Introduction

Direction of Arrival (DOA) estimation is a crucial research topic in array signal processing, finding extensive applications in various fields such as wireless communication, radar, and medical imaging. Among array structures, planar arrays are the most widely used. Over the past few decades, scholars both domestically and internationally have proposed numerous DOA estimation algorithms based on planar array structures. These include planar arrays [1], L-shaped arrays [2], and parallel linear arrays [3-5], among others. Planar arrays are typically composed of several uniformly spaced linear subarrays, possessing limited degrees of freedom. For instance, an L-shaped uniform linear array with N elements can, at most, estimate N angles of incoming signals.

In recent years, sparse arrays have gained widespread attention due to their ability to effectively increase array degrees of freedom. Examples include minimum redundancy arrays, nested arrays, and coprime arrays [6-8]. Compared to traditional arrays, sparse arrays can significantly reduce the number of elements while ensuring performance or, with the same number of elements, achieve a larger array aperture and lower side lobe levels. This is achieved by optimizing the positions and weights of array elements to improve the accuracy, resolution, and degrees of freedom direction-finding algorithms.

In the realm of sparse nested arrays, references [9-11] and [12-15] extend nested arrays from 1D DOA estimation to 2D DOA estimation, proposing a 2D nested array composed of two uniformly spaced linear subarrays. Concerning L-shaped coprime arrays, approaches based on iterative minimization and off-grid sparse learning are explored. Regarding parallel coprime arrays, reference [16-18] first introduces the construction of a 1D vector using the cross-covariance matrix of parallel coprime arrays. It improves array degrees of freedom through sparse reconstruction and least squares estimation but exhibits lower accuracy and higher algorithm complexity in scenarios with small snapshots.

To address the complexity issue, some of the algorithms transform the 2D DOA estimation problem into a 1D representation. They utilize cross-covariance matrices and compressed sensing methods for angle estimation, thereby enhancing estimation accuracy to some extent. The mentioned algorithms primarily leverage the cross-covariance matrix of parallel coprime

International Journal on Recent and Innovation Trends in Computing and Communication
ISSN: 2321-8169 Volume: 11 Issue: 11
Article Received: *10 September 2023* ***Revised:*** *20 October 2023* ***Accepted:*** *30 October 2023*

arrays. On the other hand, some algorithms use the covariance matrix of parallel coprime arrays [19-24]. They employ 1D DOA estimation combined with power matching to achieve elevation and azimuth angle estimation but are susceptible to mismatch phenomena.

It can be observed that existing parallel coprime array DOA estimation algorithms only utilize the covariance matrix or cross-covariance matrix of the array, requiring grid search and matching. This results in issues such as high computational complexity, insufficient algorithm precision, and susceptibility to mismatch. Addressing these shortcomings, this method proposes a new 2D DOA estimation algorithm based on parallel coprime linear arrays. The algorithm utilizes the covariance and cross-covariance matrices of two linear arrays to construct a new DOA estimation matrix. Building upon this, the SVD and ESPRIT algorithms are employed to obtain azimuth and elevation angles based on eigenvalues and eigenvectors. In comparison to existing algorithms, this algorithm fully utilizes autocorrelation and cross-correlation matrix information, enabling the estimation of more source signals with higher accuracy. Additionally, due to the expanded aperture of array elements, the algorithm exhibits higher resolution, lower computational complexity, and superior performance in low signal-to-noise ratio and small snapshot scenarios.

Following terminology explains the symbol used here: $(.)^T$, $(.)^*$, $(.)^H$, $(.)^{-1}$, and $(.)^+$denote matrix transpose, conjugate, conjugate transpose, inverse, and pseudo-inverse, respectively. $diag(v)$represents a diagonal matrix with vector v as its main diagonal. $vec(\cdot)$denotes matrix stretching. $\otimes$ represents the Khatri-Rao product; $\boldsymbol{I}$ denote the identity matrix; $arg(\cdot)$ represents the phase angle.

2. Signal Model

The array model in this paper adopts a parallel coprime array structure, composed of two mutually parallel extended coprime arrays, as illustrated in Figure 1, comprising Subarray 1 and Subarray 2. Subarray 1 hasN_d physical elements formed by two non- overlapping uniform linear arrays: one with element spacing $\lambda/2$and $N_d$elements, and the other with element spacing $\lambda$and $N_d$elements. Here, $N_d, 2M-1, and\ N$represent the number of elements, the number of cross elements, and the number of subarray elements, respectively. The symbols $\lambda$and $\lambda/2$represent the signal wavelength and half-wavelength, respectively. The integers $M$and $N$are coprime, and $d$is the basic element spacing. The positions of the elements within each subarray are represented by the permutation vector

$$p = \{p_0, p_1, \dots, p_{L-1}\}$$

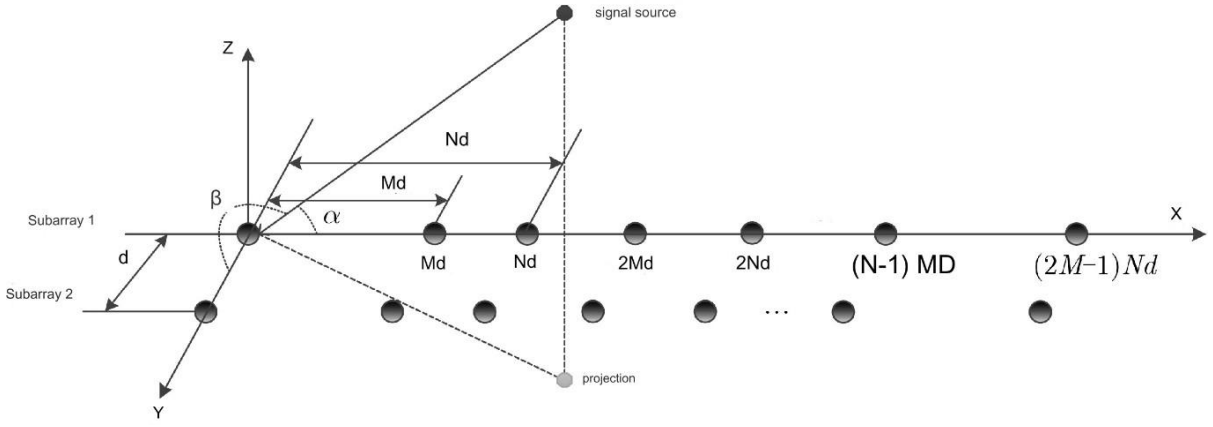

Figure4.1: Geometric model of parallel coprime array

In Figure 4.1, α and β represent the angles between the radiation source and the ϕ-axis and θ-axis, respectively, satisfying $cos\ \alpha = sin\varphi\ sin\vartheta, cos\ \beta = cos\varphi\ sin\vartheta$. Here, α and β denote the azimuth and elevation angles of the radiation source. When there are Kfar-field narrowband incoming signals, the signal model received by the l^{th}element of Subarray1 can be expressed as:

International Journal on Recent and Innovation Trends in Computing and Communication
ISSN: 2321-8169 Volume: 11 Issue: 11
Article Received: *10 September 2023* ***Revised:*** *20 October 2023* ***Accepted:*** *30 October 2023*

$$z_{1,l}(t) = \sum_{k=1}^{K} e^{j2\pi d/\lambda_{pl}\cos(\alpha_k s_k(t)} + n_{1,l}(t),\ \ l - 0,1,\dots,L \ ---(4.1)$$

Here, $s_k(t)$ represents the amplitude of the k^{th}incoming signal, and $n_{1,l}(t)$is the noise term. The overall signal model for the entire array is given by:

$$z_1(t) = As(t) + n_1(t) ----(4.2)$$

$$z_2(t) = A\phi s(t) + n_2(t) ----(4.3)$$

where A is the array response matrix, $s(t)$is the vector of amplitudes of K signals, and $n_1(t)$and$n_2(t)$ are the noise terms for Subarray 1 and Subarray 2, respectively.

$$\boldsymbol{A} = [\boldsymbol{a_1}, \boldsymbol{a_2}, \dots., \boldsymbol{a_k}]$$

$$\boldsymbol{a_k} = [1, e^{\frac{j2\pi d}{\lambda_{p1}\cos(\alpha_k)}}, e^{\frac{j2\pi d}{\lambda_{p2}\cos(\alpha_k)}}, \dots, e^{\frac{j2\pi d}{\lambda_{pL-1}\cos(\alpha_k)}}]^{\mathrm{T}}$$

The dimensions of the direction matrix Φ are L×2, including the azimuth and elevation angle information of the incoming signals, and the response vector corresponds to the k^{th}incoming signal. The amplitudes s_k represent the amplitude of the non-cooperative narrowband signals, $n_1$and n_2 denote zero-mean additive white Gaussian noise, with noise and signals being uncorrelated.

$$\boldsymbol{\phi} = diag(e^{-j\pi\cos(\beta_1)}, e^{-j\pi\cos(\beta_2)}, \dots., e^{-j\pi\cos(\beta_k)})_{K\,\mathrm{X}\,K}$$

Where $\alpha_1 \neq \alpha_2 \neq \alpha_3 \neq \cdots \neq \alpha_kand\beta_1 \neq \beta_2 \neq \beta_3 \neq \cdots \neq \beta_k$ and $\boldsymbol{\phi}$ is a diagonal matrix. Here, it is assumed that all incoming signals do not overlap, i.e., $\alpha_i \neq \alpha_j$and $\beta_i \neq \beta_j$for all $i \neq j$. In the array model with L antennas (where L=2M−1+N), the degrees of freedom are enhanced due to the use of extended coprime subarrays in forming a parallel array. By

constructing virtual domain signals, when there are M physical elements in a single subarray, the number of consecutive virtual elements can be 2M−1, yielding a total degree of freedom of $2MN + 2M - 1$. This breakthrough overcomes the traditional limitation of the physical elements in an array, effectively expanding the antenna aperture and increasing the degrees of freedom for DOA estimation.

3. Low-Complexity2DDOAEstimationAlgorithmBasedonParallelCoprime Virtual Arrays

As mentioned earlier, existing 2D DOA estimation algorithms suffer from issues such as high computational complexity, insufficient accuracy, and susceptibility to mismatch. In response to these challenges, this study focuses on investigating 2D virtual arrays, proposing a 2D DOA estimation algorithm tailored for parallel coprime virtual arrays.

Extended Matrix Construction

Considering the received data of incoming signals, the first step is to construct a DOA extensionmatrixapplicableto2Dvirtualarrayestimation.Thecovariance matrix of Sub array 1's received signals $\boldsymbol{z_1} = \boldsymbol{z_1}(t)$(at a specific time t) is given by:

$$\boldsymbol{R_b} = E[z_1 z_1{}^H] = \boldsymbol{ARA^H} + z_1\sigma_n^2\boldsymbol{I} ----(4.4)$$

where $\boldsymbol{R} = diag(\rho_1, \rho_2, \dots\dots, \rho_K), \rho_K(k = 1,2, \dots, K)$is a diagonal matrix with signal powers ρ_1, ρ_2, ……, ρ_K and σ_n^2 denotes the noise power. Vectorizing$\boldsymbol{R_b}$ yields:

International Journal on Recent and Innovation Trends in Computing and Communication
ISSN: 2321-8169 Volume: 11 Issue: 11
Article Received: *10 September 2023* ***Revised:*** *20 October 2023* ***Accepted:*** *30 October 2023*

$$\boldsymbol{v_1} = vec(\boldsymbol{R_b}) = \boldsymbol{B_r} + \sigma_n^2 \boldsymbol{I_e} - - - -(4.5)$$

Here, $\boldsymbol{B}$ is a matrix involving array response vectors a_k, $r$is a vector containing signal powers, and $\boldsymbol{I_e}$is the vectorized identity matrix.

$$\boldsymbol{B} = [\boldsymbol{a_1} \otimes \boldsymbol{a_1^*}, \boldsymbol{a_2} \otimes \boldsymbol{a_2^*}, \dots, \boldsymbol{a_k} \otimes \boldsymbol{a_k^*}]$$

$$r = [\rho_1, \rho_2, \rho_3, \dots, \rho_k]^T, \boldsymbol{I_e} = vec(\boldsymbol{I})$$

$$\bar{\boldsymbol{v}}_1 = \boldsymbol{v}_1 - \sigma_n^2 \boldsymbol{I}_n - - - -(4.6)$$

Next, considering that there are duplicate elements in, it needs to be eliminated by repeating elements and intercepting consecutive virtual array elements, you can get $2M-1$ located in $\{-(MN+M-1), -(MN+M-2), \dots, -1, 0, 1, \dots, (MN+M-2), (MN+M-1)\}$ array elements at the position,

$$\bar{\boldsymbol{v}}_{\boldsymbol{1}} = \left[\bar{v}_{-(MN+M-1)}, \bar{v}_{-(MN+M-2)}, \dots, \bar{v}_{-1}, \bar{v}_0, \bar{v}_1, \dots, \bar{v}_{(MN+M-2)}, \bar{v}_{(MN+M-1)}\right] = \bar{\boldsymbol{B}}_r - - - -(4.7)$$

$$\bar{\boldsymbol{B}} = [\bar{\boldsymbol{B}}_1, \bar{\boldsymbol{B}}_2, \dots, \bar{\boldsymbol{B}}_K], \bar{\boldsymbol{B}}_K = \left[e^{j\pi(MN+M-1)\cos\alpha k}, e^{j\pi(MN+M-2)\cos\alpha k}, \dots, 0, e^{-j\pi\cos\alpha k}, \dots, e^{-j\pi(MN+M-1)\cos\alpha K}\right]$$

Here,$\bar{v}_1$ represents the modified vector,$\bar{\boldsymbol{B}}$is a matrix, and$\bar{\boldsymbol{B}}_K$is a vector for the k^{th}incoming signal. By rearranging the elements of the vector , we obtain the matrix:

$$V_1 = \begin{bmatrix} \bar{v}_0 & \bar{v}_{-1} & \cdots & \bar{v}_{-(MN+M-1)} \\ \bar{v}_1 & \bar{v}_0 & \ddots & \bar{v}_{-(MN+M-2)} \\ \vdots & \vdots & & \vdots \\ \bar{v}_{(MN+M-1)} & \bar{v}_{(MN+M-2)} & \cdots & \bar{v}_0 \\ \vdots & & & \end{bmatrix} - -(4.8)$$

Here, the dimensions of the matrix $\boldsymbol{V}_1$are $(MN+M)\times(MN+M)$.Matrix V_1can be expressed as:

$$\boldsymbol{V_1} = \boldsymbol{D}\boldsymbol{W}(\rho)\boldsymbol{D}^H - - - -(4.9)$$

where W is a diagonal matrix related to the signal powers, and D contains information about the angles between incoming signals and the X-axis. Similarly, by defining the cross- covariance matrix for Subarray 1 and Subarray 2 using the received signals:

$$\boldsymbol{R_c} = E[z_1(t){z_2}^H(t)] = \boldsymbol{A}\boldsymbol{\phi}\boldsymbol{R}\boldsymbol{A}^{\boldsymbol{H}} - - - -(4.10)$$

Where$\phi = diag(e^{-j\pi\cos\beta 1}, e^{-j\pi\cos\beta 2}, \dots, e^{-j\pi\cos\beta K})$,and $\boldsymbol{R_c}$ contains information about the angles between incoming signals and the Y-axis. Since the noise in the two subarrays is uncorrelated the cross-covariance matrix has no noise interference. Vectorizing $\boldsymbol{R_c}$ yields:

$$\boldsymbol{v_2} = vec(\boldsymbol{R_c}) = B\phi r - - - - - (4.11)$$

Similarly, removing duplicate elements from $\boldsymbol{v_2}$and selecting continuous virtual elements, we get:

International Journal on Recent and Innovation Trends in Computing and Communication
ISSN: 2321-8169 Volume: 11 Issue: 11
Article Received: *10 September 2023* ***Revised:*** *20 October 2023* ***Accepted:*** *30 October 2023*

$$\bar{v}_2 = \bar{B}\phi r \quad -----(4.12)$$

Constructing the cross-covariance matrix, i.e., rearranging the elements of $\bar{v}_2$,results in:

$$V_2 = D\phi W(\rho)D^H \quad ----(4.13)$$

Combining the matrices $V_1$and $V_2$with the original matrix **V** (from Equation 4.8) yields the extended matrix for DOA estimation:

$$R_m = \begin{bmatrix} V_1 \\ V_2 \end{bmatrix} = \begin{bmatrix} DW(\rho)D^H \\ D\phi W(\rho)D^H \end{bmatrix}$$

$$= \begin{bmatrix} D \\ D\phi \end{bmatrix} = W(\rho)D^H = DW(\rho)D^H \quad ----(4.14)$$

Analysis of $R_m$shows that D includes the incident signal and the X-axis and all the information about the angle between the Y axis, that is, D is the required matrix. $R_m$is the signal subspace obtained through singular value decomposition (SVD) of $\bar{D}$, we obtain the signal subspace, which spans the desired space.

2DDOA Estimation

In the above Section, the DOA estimation matrix was constructed using the covariance matrix of Subarray 1 and its cross-covariance matrix with Subarray 2. Now, utilizing the Singular Value Decomposition (SVD) and ESPRIT algorithm, this study extracts matching azimuth and elevation angles from the eigenvalues and eigenvectors. Firstly, performing SVD on the DOA estimation matrix$R_m$yields:

$$R_m = [U_1 \;\; U_2]\begin{bmatrix} \Sigma & 0 \\ 0 & 0 \end{bmatrix} V^H \quad ----(4.15)$$

Here,U_1 represents the signal subspace, and$U_2$is the noise subspace. The matrices U_1 and U_2can be expressed as:

$$U_1 = [u_1; u_2; \ldots.; u_k] \quad -----(4.16)$$

$$U_2 = [u_{K+1}; u_{K+2}; \ldots.; u_{MN+M}] \quad -----(4.17)$$

U_1 is a matrix of size $2(MN + M) \times K$, where $K$is the number of incident signals. Since $U_1$is the signal subspace, there exists a $K \times K$matrix Tsuch that equation (4.17) holds.

As $U_1$is the signal subspace, it can be expressed as

$$U_1 = \begin{bmatrix} U_{11} \\ U_{12} \end{bmatrix} = \begin{bmatrix} D \\ D\phi \end{bmatrix} T = \bar{D}T \quad ----(4.18)$$

Where D contains the angles between the incoming signals and the X-axis. From the analysis above, it is evident that the signal subspace contains information about the azimuth and elevation angles of incoming signals. Here, D represents the direction matrix containing information about the angles between incoming signals and the Y-axis, and **Φ** is the diagonal matrix containing information about the angles between incoming signals and the X-axis. This leads to:

International Journal on Recent and Innovation Trends in Computing and Communication
ISSN: 2321-8169 Volume: 11 Issue: 11
Article Received: *10 September 2023* ***Revised:*** *20 October 2023* ***Accepted:*** *30 October 2023*

$$\boldsymbol{U_{11} = DT} - - - -(4.19)$$

$$\boldsymbol{U_{12} = D\Phi T} - - - -(4.20)$$

Here,$\boldsymbol{U}_{11}$and $\boldsymbol{U}_{12}$are both $(MN + M) \times K$matrices. By establishing a relationship between $\boldsymbol{U}_{11}$ and $\boldsymbol{U}_{12}$, a matrix $\boldsymbol{F}$ is constructed:

$$\boldsymbol{F = U_{11}^{+} U_{12} = T^{-1}\Phi T} - - - -(4.21)$$

This allows obtaining the corresponding eigenvalues $\{\Psi_K, K = 1.2. \dots, K\}$and, consequently, the angles between the incoming signals and the Y-axis:

$$\hat{\beta}_k = cos^{-1}\left(\frac{\arg(\Psi_K)}{2\pi/_{\lambda}}\right) - - - -(4.22)$$

By performing eigenvalue decomposition on Equation (4.20), the corresponding eigenvectors form the matrix T, and using Equation (4.18), we get:

$$\widehat{\boldsymbol{D}} = \boldsymbol{U_{11}T^{-1}} - - - -(4.23)$$

Here,$\widehat{\boldsymbol{D}}$is an $(MN + M) \times K$matrix, by constructing a spectral peak search function for angle search, and then obtain the angle between the incident signal and the X-axis, algorithm complexity is high and efficiency is low. This method draws on the idea of rotation invariance and combines. Divide the matrix into blocks and take the1st row of the matrix to a row, take the 2nd row of the matrix to another row.

Angle search is performed by constructing a spectral peak search function, and then the angle between the incident signal and the X-axis is obtained. The algorithm is highly complex and has lower efficiency than $\widehat{\boldsymbol{D}}$. This article draws on the idea of rotation invariance, divides the matrix into blocks, and $\boldsymbol{C}_1$takes the matrix $\widehat{\boldsymbol{D}}$ first row to $(MN + M - 1)$rows,$\boldsymbol{C_2}$ takes the 2nd row to$MN + M$rows of matrix $\widehat{\boldsymbol{D}}$, then we have

$$\boldsymbol{C_2 = C_1\Psi} - - - -(4.24)$$

Among them, $\boldsymbol{\Psi} = diag(e^{j\pi \cos \alpha 1}, e^{j\pi \cos \alpha 2}, \dots, e^{j\pi \cos \alpha K})$, which is the spin, Transform into invariant factors, then we have,

$$\boldsymbol{\Psi = C_1^{-1} C_2} - - - -(4.25)$$

By performing eigenvalue decomposition on Ψ, the eigenvalue $\gamma_K$is obtained, then there is

$$\hat{\alpha}_k = cos^{-1}\left(\frac{\arg(\gamma_K)}{2\pi/_{\lambda}}\right), k = 1,2, \dots, K - - - -(4.26)$$

Through the combination of Equation (4.21) and Equation (4.25), the azimuth angle and pitch angle that match each other can be obtained, that is

International Journal on Recent and Innovation Trends in Computing and Communication
ISSN: 2321-8169 Volume: 11 Issue: 11
Article Received: *10 September 2023* ***Revised:*** *20 October 2023* ***Accepted:*** *30 October 2023*

$$\theta_k = sin^{-1}(\sqrt{cos^2(\hat{\alpha}_k) + cos^2(\hat{\beta}_k)} - - - -(4.27)$$

$$\varphi_k = tan^{-1}\left(\frac{cos(\hat{\alpha}_k)}{cos(\hat{\beta}_k)}\right) - - - -(4.28)$$

Algorithm Steps

Based on the theoretical analysis presented above, here are the specific steps of the algorithm proposed in this method:

Step 1: Estimate the covariance matrix and cross-covariance matrix using a finite number of snapshots, denoted by P:

$$\widehat{\boldsymbol{R}}_{\boldsymbol{b}} = \frac{1}{P}\sum_{p=1}^{P} z_1(t){z_1}^H(t);\ \ n = 1,2,\dots,P - - - -(4.29)$$

$$\widehat{\boldsymbol{R}}_{\boldsymbol{c}} = \frac{1}{P}\sum_{p=1}^{P} z_1(t){z_2}^H(t);\ \ n = 1,2,\dots,P - - - -(4.30)$$

Step2: Construct a new DOA estimation matrix$\boldsymbol{R}_m$using$\widehat{\boldsymbol{R}}_{\boldsymbol{b}}and\widehat{\boldsymbol{R}}_{\boldsymbol{c}}$.

Step 3: Perform Singular Value Decomposition (SVD) on the matrix $\boldsymbol{R}_m$to obtain the signal subspace.

Step 4: Construct an angle estimation matrix $\boldsymbol{\Psi}$ to find the radiation source angle information.

Step 5: Utilize the ESPRIT concept to construct a rotation factor containing azimuth information and estimate the radiation source angle information.

Step 6: Obtain the azimuth and elevation angles of the incident signals using Equations (4.26) and (4.27).

The complexity of the algorithm mainly involves the construction of covariance and cross-covariance matrices, Eigenvalue Decomposition (EVD), and Singular Value Decomposition (SVD). After derivation, the algorithm's complexity is approximately $O\{2L^2P + 2K^3 + (2MN + 2M)^3\}$, where $L = 2M - 1 + N$, P is the number of sampled snapshots, M and N are coprime numbers, and K is the number of incident signals.

The proposed algorithm utilizes the concept of coprime virtual arrays to extend 2D parallel arrays. This allows for estimating more incident angles with a limited number of array elements. Additionally, due to the extension of the array aperture, it provides better resolution for incident angles. The algorithm demonstrates relatively higher accuracy, especially in low Signal-to-Noise Ratio (SNR) and small snapshot scenarios, and exhibits lower computational complexity.

4. Experimental Simulation and analysis

In this section, the experimental simulation is conducted with $M = 3$and $N = 5$, making the actual number of elements in Subarray 1, $L = 10$. The array elements are positioned at $[0,3,5,6,9,10,12,15,20,25]$.Considering multiple incident signals, the numberof signal sources is set to $K = 11$. The traditional parallel linear array algorithms become ineffective in this scenario, whereas the proposed algorithm can still effectively estimate the incident angles, as shown in Figure 4.2. The algorithm efficiently extends the array aperture, improving the utilization of array elements and allowing estimation of up to 11 incident angles, surpassing traditional algorithms.

To further verify the high-resolution performance of the proposed algorithm, assume the number of incident signals is two, with incident angles $\theta = 10°$and$\theta = 11°$. In this case, traditional algorithms fail, while the experimental results of the proposed algorithm, as shown in Figure 4.3, demonstrate that despite some error, it can still distinguish two very close incident angles. It is important to note that, due to the proximity of angles, the experiment requires a high Signal-to-Noise Ratio (SNR) and a sufficient number of snapshots.

Evaluation Criterion

International Journal on Recent and Innovation Trends in Computing and Communication
ISSN: 2321-8169 Volume: 11 Issue: 11
Article Received: *10 September 2023* ***Revised:*** *20 October 2023* ***Accepted:*** *30 October 2023*

To assess the algorithm's estimation accuracy, this algorithm employs the Root Mean Square Error (RMSE) criterion, defined as follows:

$$RMSE = \frac{1}{K}\sum_{k=1}^{K}\sqrt{\frac{1}{Q}\sum_{q=1}^{Q}(\hat{\phi}_{k;q}-\phi_k)^2+(\hat{\theta}_{k;q}-\theta_k)^2} - - - -(4.31)$$

Here, K represents the number of incident signals, Q denotes the Monte Carlo experiment count, $\hat{\phi}_{k;q}$and $\hat{\theta}_{k;q}$are the DOA estimates for the q^{th}experiment of the k^{th}incident signal.

Influence of Snapshot Number

Figure 4 illustrates the impact of the number of snapshots on the performance of the algorithm proposed in this paper, comparing it with existing algorithms. In this comparison, proposed algorithm with Spatial Smoothing-Multiple Signal Classification (SS- MUSIC)[131], Alternating projection- Multiple Signal Classification (AP-MUSIC)[132] algorithm ADMM algorithm [133]. Considering the application scope of existing algorithms, estimation is performed for four signal sources with incident angles of$(10°,10°),(20°,20°),(30°,30°),and\ (40°,40°)$.It can be observed that the proposed algorithm exhibits good estimation performance even with a small number of snapshots. Notably, when the number of snapshots $P = 10$, the proposed algorithm can still achieve effective DOA estimation, making it suitable for scenarios with a limited number of snapshots.

Influence of Signal-to-Noise Ratio (SNR)

Next, the impact of varying Signal-to-Noise Ratio (SNR) on the performance of various algorithms is analysed, assuming a large number of snapshots ($P = 500$)to minimize the effect of snapshot numbers. The experiment includes the same incident signal conditions as in Figure 4.4. As shown in Figure 4.5, the proposed algorithm maintains high estimation accuracy even in low SNR conditions.

5. Computational Complexity Analysis

Finally, a comparison analysis of the computational complexity of different DOA estimation algorithms is conducted. Under the same hardware and software conditions, 600 Monte Carlo experiments are performed to record the runtime of each algorithm. The CPU used in the experiment is an I7-8550U, with 8 GB of RAM. The conditions for incident signals are the same as in Figures 4.3 and 4.4, with $P = 500$snapshots and $SNR = 20\,dB$. The statistical results are presented in Table 1, indicating that the computational complexity of the proposed algorithm is superior to rest of the three existing algorithms.

Table1 Run time of Different 2DDOA Estimation Algorithms(seconds)Estimation Algorithm Runtime

Sl#	Algorithm	Runningtime
1	ADMM	0.0189
2	AP-MUSIC	0.0598
3	SS-MUSIC	0.0040
4	PCVA	0.0034

International Journal on Recent and Innovation Trends in Computing and Communication
ISSN: 2321-8169 Volume: 11 Issue: 11
Article Received: *10 September 2023* ***Revised:*** *20 October 2023* ***Accepted:*** *30 October 2023*

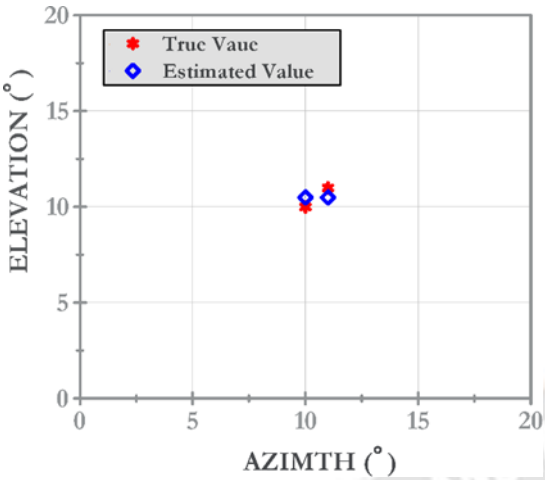

Figure4.2Algorithm estimation results when K=11(SNR=4dB,P=200)

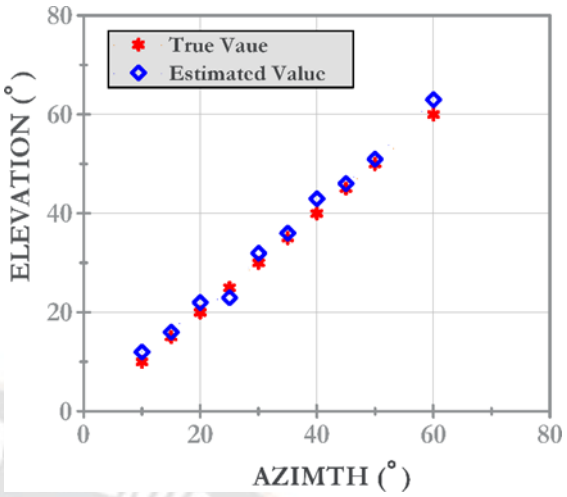

Figure4.3 High-resolution experiment (K=2,SNR=4dB,P=200)

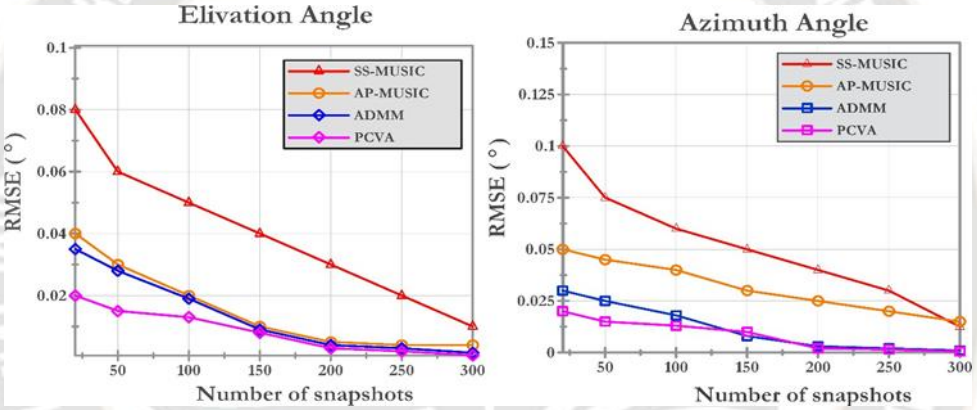

Figure 4.4 Performance comparison of algorithms with the different snapshot number (K=4, SNR=4 dB)

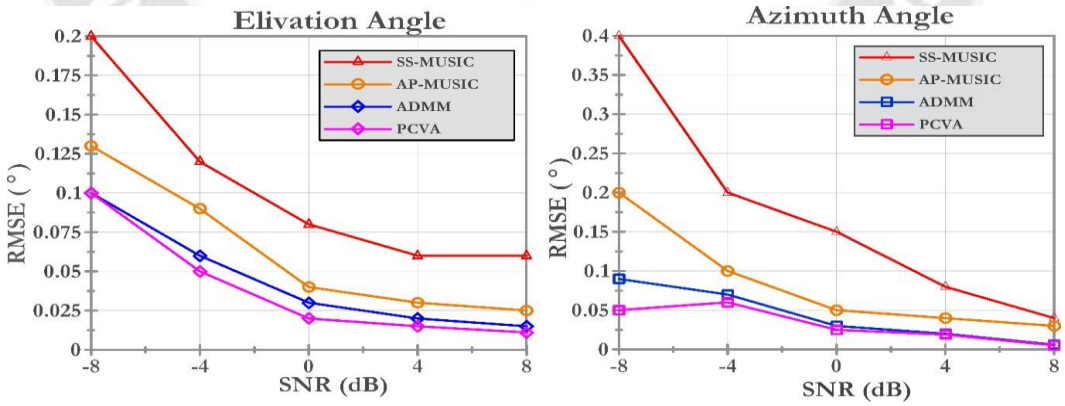

Figure 4.5 Performance analysis under different signal-to-noise ratios (K=4,P=200)

6. Conclusion :

This Paper introduces a low-complexity 2D Direction of Arrival (DOA) estimation algorithm based on parallel coprime virtual arrays, combining traditional parallel linear arrays with coprime virtual arrays. The extended DOA matrix is utilized in the estimation process, leveraging Singular Value Decomposition (SVD) and extracting rotation-invariant factors. This approach avoids the spectral peak search used in traditional algorithms, reducing algorithm complexity and obtaining automatically matched DOA estimates. Additionally, the virtual array is employed to extend the array aperture, addressing the issue of

traditional DOA estimation algorithms having fewer incident signal sources than actual physical array elements. Simulation results demonstrate that the proposed algorithm has higher resolution, capable of distinguishing more radiation source signals. Moreover, it outperforms traditional DOA estimation algorithms, especially in scenarios with low SNR and a small number of snapshots.

References

[1] X. D. Qian and S. G. Jin, "Estimation of snow depth from GLONASS SNR and phase-based multipath reflectometry," IEEE J. Sel. Topics Appl. Earth Obs. Remote Sens., vol. 9, no. 10, pp. 4817–4823, Oct. 2016.

[2] V.U.Zavorotny,K.M.Larson,J.J.Braun,E.E.Small,E.D.Gutmann,and
A. L. Bilich, "A physical model for GPS multipath caused by land reflections: Toward bare soilmoistureretrievals,"IEEEJ.Sel.TopicsAppl.EarthObs.RemoteSens.,vol.3,no.1,
pp.100–110,Oct.2010.

[3] F. G. Nievinski, M. F. Silva, K. Boniface, and J. F. G. Monico, "GPS diffractive reflectometry: Footprint of a coherent radio reflection inferred from the sensitivity kernel of multipath SNR," IEEEJ. Sel. Topics Appl. EarthObs. RemoteSens., vol. 9, no. 10,
pp.4884–4891,Oct.2016.[4] A. V. Mrstik and P. G. Smith, "Multipath limitations on low-angle radar tracking," IEEE Trans. Aerosp. Electron. Syst., vol. 14, no. 1, pp. 85–102, Jan. 1978.

[5] PAL P and VAIDYANATHAN P P. Nested arrays in two dimensions, part I: Geometrical considerations. IEEE Transactions on Signal Processing, 2012, 60(9): 4694– 4705. doi: 10.1109/TSP.2012.2203814.

[6] Carlin M, Rocca P, Oliveri G, et al. Direction-of-arrival estimation through Bayesian compressive sensing strategies. IEEE Transactions on Antennas and Propagation, 2013, 61(7): 3828-3838.

[7] X. D. Qian and S. G. Jin, "Estimation of snow depth from GLONASS SNR and phase-based multipath reflectometry," IEEE J. Sel. Topics Appl. Earth Obs. Remote Sens., vol. 9, no. 10, pp. 4817–4823, Oct. 2016.

[8] F. G. Nievinski, M. F. Silva, K. Boniface, and J. F. G. Monico, "GPS diffractive reflectometry: Footprint of a coherent radio reflection inferred from the sensitivity kernel of multipath SNR," IEEEJ. Sel. Topics Appl. EarthObs.RemoteSens., vol. 9, no. 10,
pp.4884–4891,Oct.2016.

[9] LAVATE TB, KOKATE VK, and SAPKAL A M. Performance analysis of MUSIC and ESPRIT DOA estimation algorithms for adaptive array smart antenna in mobile communication[C]. The 2010 Second International Conference on Computer and Network Technology, Bangkok, Thailand, 2010: 308-311. doi: 10.1109/ICCNT. 2010.45.

[10] LIU Yuan, LIU Hongwei, XIA Xianggen,et al. Projection techniques for altitude estimation over complex multipath condition-based VHF radar.IEEE Journal of Selected Topics in Applied Earth Observations and Remote Sensing, 2018, 11(7): 2362–2375. doi:10.1109/JSTARS.2018.2835448.

[11] Sanjeev Kumar Machkuri, Y Ravi Kumar, A Novel two-dimensional DOA Estimation Algorithm for Low Elevation Targets, Tuijin Jishu/Journal of Propulsion Technology, ISSN: 1001-4055, Vol. 44 No. 4 (2023):3902-39012.

[12] Thatikonda, R., Vaddadi, S. A., Arnepalli, P. R., &Padthe, A. (2023). Securing biomedical databases based on fuzzy method through blockchain technology. *Soft Computing*. https://doi.org/10.1007/s00500-023-08355-x , **(Publisher: Springer Link)**

[13] Mythili, R., bama, B. S., Kumar, P. S., Das, S., Thatikonda, R., &Inthiyaz, S. (2023). Radial basis function networks with Lightweight Multiscale Fusion strategy-based underwater image enhancement. *Expert Systems*. https://doi.org/10.1111/exsy.13373, **(Publisher: Wiley)**

[14] Vaddadi, S. A., Thatikonda, R., Padthe, A., &Arnepalli, P. R. (2023). *Shift-Left Testing Paradigm Process Implementation for Quality of Software Based on Fuzzy*. https://doi.org/10.21203/rs.3.rs-2845536/v1, **(Publisher: Springer Link)**

[15] Vishwakarma, S., Goswami, R. S., Nayudu, P. P., Sekhar, K. R., Arnepalli, P. R., Thatikonda, R., & Abdel-Rehim, W. M. (2023). Secure Federated Learning Architecture for fuzzy classifier in healthcare environment. Soft Computing. https://doi.org/10.1007/s00500-023-08629-4 - (Publisher: Springer Link)

[16] Naga Simhadri Apparao Polireddi, K Chaitanya, Web accessibility evaluation of private and government websites for people with disabilities through fuzzy classifier in the USA, Soft Computing, Pages 1-9. 2023.

[17] Adithya Padthe Srinivas Aditya Vaddadi , Pandu Ranga Rao Arnepalli , RamyaThatikonda, , Effective Malware Detection Approach based on Deep Learning in Cyber-Physical Systems, International Journal of Computer Science and Information Technology, Volume 14, Issue 6, Pp 01-12.

[18] Naga Simhadri Apparao Polireddi, Krovi Raja Sekhar, Improved fuzzy-based MCDM–TOPSIS model to find and prevent the financial system vulnerability and hazards in real time, Soft Computing, 1-8.

[19] R Pulimamidi, GP Buddha, Applications of Artificial Intelligence Based Technologies in The Healthcare Industry, Tuijin Jishu/Journal of Propulsion Technology 44 (3), 4513-4519.

[20] R Pulimamidi, GP Buddha, AI-Enabled Health Systems: Transforming Personalized Medicine And Wellness, Tuijin Jishu/Journal of Propulsion Technology 44 (3), 4520-4526.
[21] R Pulimamidi, P Ravichandran, Connected Health: Revolutionizing Patient Care Through Artificial Intelligence Innovations, Tuijin Jishu/Journal of Propulsion Technology 44 (3), 3940-3947.
[22] R Pulimamidi, P Ravichandran, Enhancing Healthcare Delivery: AI Applications In Remote Patient Monitoring, Tuijin Jishu/Journal of Propulsion Technology 44 (3), 3948-3954.
[23] Ramya Manikyam, J. Todd McDonald, William R. Mahoney, Todd R. Andel, and Samuel H. Russ. 2016.Comparing the effectiveness of commercial obfuscators against MATE attacks. In Proceedings of the 6th Workshop on Software Security, Protection, and Reverse Engineering (SSPREW'16)
[24] R. Manikyam. 2019.Program protection using software based hardware abstraction.Ph.D. Dissertation.University of South Alabama.